Neuromechanical coupling within the human triceps surae and its consequence on individual force sharing strategies

Marion Crouzier, Lilian Lacourpaille, Antoine Nordez, Kylie Tucker, François Hug

RESEARCH ARTICLE

Neuromechanical coupling within the human triceps surae and its consequence on individual force-sharing strategies

Marion Crouzier[1], Lilian Lacourpaille[1], Antoine Nordez[1,2], Kylie Tucker[3] and François Hug[1,4,5,*]

ABSTRACT

Little is known about the factors that influence the coordination of synergist muscles that act across the same joint, even during single-joint isometric tasks. The overall aim of this study was to determine the nature of the relationship between the distribution of activation and the distribution of force-generating capacity among the three heads of the triceps surae [soleus (SOL), gastrocnemius medialis (GM) and gastrocnemius lateralis (GL)]. Twenty volunteers performed isometric plantarflexions, during which the activation of GM, GL and SOL was estimated using electromyography (EMG). Functional muscle physiological cross-sectional area (PCSA) was estimated using imaging techniques and was considered as an index of muscle force-generating capacity. The distribution of activation and PCSA among the three muscles varied greatly between participants. A significant positive correlation between the distribution of activation and the distribution of PCSA was observed when considering the two bi-articular muscles at intensities ≤50% of the maximal contraction ($0.51<r<0.62$). Specifically, the greater the PCSA of GM compared with GL, the stronger bias of activation to the GM. There was no significant correlation between monoarticular and biarticular muscles. A higher contribution of GM activation compared with GL activation was associated with lower triceps surae activation ($-0.66<r<-0.42$) and metabolic cost ($-0.74<r<-0.52$) for intensities ≥30% of the maximal contraction. Considered together, an imbalance of force between the three heads was observed, the magnitude of which varied greatly between participants. The origin and consequences of these individual force-sharing strategies remain to be determined.

KEY WORDS: Muscle coordination, Calf, Achilles tendon, Activation, Electromyography

INTRODUCTION

Coordination at multiple levels, e.g. between muscles within a synergistic group, over one or more joints, and between limbs, is required to achieve the vast majority of movements. With multiple muscles able to act upon the same joint, many different muscle coordination strategies are theoretically possible to achieve the same motor goal (Diedrichsen et al., 2010; Kutch and Valero-Cuevas, 2011). Force sharing among synergistic muscle groups has been studied extensively in animal models as well as with biomechanical models (reviewed in Herzog, 2000, 2017). Even though these works provided substantial insight into muscle coordination strategies, they did not identify the factors that influence the coordination of synergist muscles that act across the same joint, even during simple isometric tasks. Addressing this issue is fundamental to understanding the control of movement, and requires knowledge of the relationship between the activation a muscle receives and its force-generating capacity.

Large inter-individual variability in the distribution of force-generating capacity exists among synergist muscles. For example, the ratio of physiological cross-sectional area (PCSA) between the vastus lateralis (VL) and vastus medialis (VM) measured on 12 human cadavers varied between 47.3 and 68.3% (Farahmand et al., 1998). It is unclear how the nervous system accounts for these individual differences in force-generating capacity. There are several hypotheses. First, activation is equally shared between synergist muscles, in which case the imbalance of force would match the imbalance of force-generating capacity (solution 1, Fig. 1). Second, the force sharing strategy is similar among individuals with either balanced or imbalanced force between synergist muscles. In this latter case, the distribution of activation would vary between individuals (solution 2, Fig. 1). Third, the muscle with the higher force-generating capacity receives greater activation, in which case the overall activation would be reduced but a large imbalance of force would exist [solution 3; supported by some biomechanical models (Crowninshield and Brand, 1981), Fig. 1]. Finally, it is possible that there is no specific coupling between activation and force-generating capacity (solution 4, not shown in the figure).

Hug et al. (2015) reported a large positive correlation between the ratio of muscle activation [quantified using electromyography (EMG)] and the ratio of muscle force-generating capacity (i.e. the muscle PCSA) in two synergist muscles of the thigh (VL and VM). Specifically, individuals with greater force-generating capacity of VL compared with VM exhibited a stronger bias of activation to VL. However, interpretations of this neuromechanical coupling in terms of motor control principles and biomechanical consequences remain unclear. First, it is likely that this coupling contributed to reduce the average activation of the whole muscle group, leading to a lower effort (Fig. 1). However, owing to limitations of measuring activation of the deep vastus intermedius muscle through surface electrodes, this hypothesis has not been tested. Second, the neuromechanical coupling reported by Hug et al. (2015) logically led to a force imbalance between the VM and VL, the magnitude of which varied greatly between participants. However, the quadriceps muscle is not an ideal model to understand the mechanical effect of this force imbalance on the non-muscular structures. This is because a force imbalance between the VL and VM can be counterbalanced at the joint level by different moment arms. In addition, the

[1]University of Nantes, Laboratory 'Movement, Interactions, Performance' (EA 4334), Faculty of Sport Sciences, 44000 Nantes, France. [2]Health and Rehabilitation Research Institute, Faculty of Health and Environmental Sciences, Auckland University of Technology, Auckland, 1010 New Zealand. [3]The University of Queensland, School of Biomedical Sciences, Brisbane, Queensland 4072, Australia. [4]The University of Queensland, NHMRC Centre of Clinical Research Excellence in Spinal Pain, Injury and Health, School of Health and Rehabilitation Sciences, Brisbane, Queensland 4072, Australia. [5]Institut Universitaire de France (IUF), 75231 Paris, France.

*Author for correspondence (francois.hug@univ-nantes.fr)

F.H., 0000-0002-6432-558X

Received 20 June 2018; Accepted 12 September 2018

List of abbreviations

EMG	electromyography
Gas	gastrocnemii
GL	gastrocnemius lateralis
GM	gastrocnemius medialis
MVC	maximal voluntary contraction
PCSA	physiological cross-sectional area
RMS	root mean square
SOL	soleus
TS	triceps surae
VL	vastus lateralis
VM	vastus medialis

difference in PCSA between the VL and VM is moderate. It is unclear how the activation is distributed between synergist muscles with a much larger difference in force-generating capacity. If such a coupling persists, a dramatic imbalance of muscle force would be observed. This imbalance could have important mechanical effects on the soft tissues and joint structures, with either positive (e.g. adaptation in mechanical properties, tissue remains functional) or negative consequences (pathological changes in the tissues).

The human triceps surae is an ideal muscle group to provide insight into the coordination of synergist muscles that act across the same joint. First, activation of each of the three heads of the triceps surae [gastrocnemius medialis (GM), gastrocnemius lateralis (GL) and soleus (SOL)] can be measured using surface EMG. Second, each head is connected to a fascicle bundle of the same tendon, the Achilles tendon (Szaro et al., 2009). As such, an imbalance of force between the three heads is likely to have mechanical effect on the tendon, as suggested in cadaver preparations (Arndt et al., 1999) and from computational modelling (Handsfield et al., 2016). Third, the three heads of the triceps surae have large differences in PCSA; i.e. GM PCSA is 2.1 times larger than that of GL, and SOL PCSA is 2.6 and 5.5 times larger than that of GM and GL, respectively (Albracht et al., 2008). Finally, this muscle group is composed of two

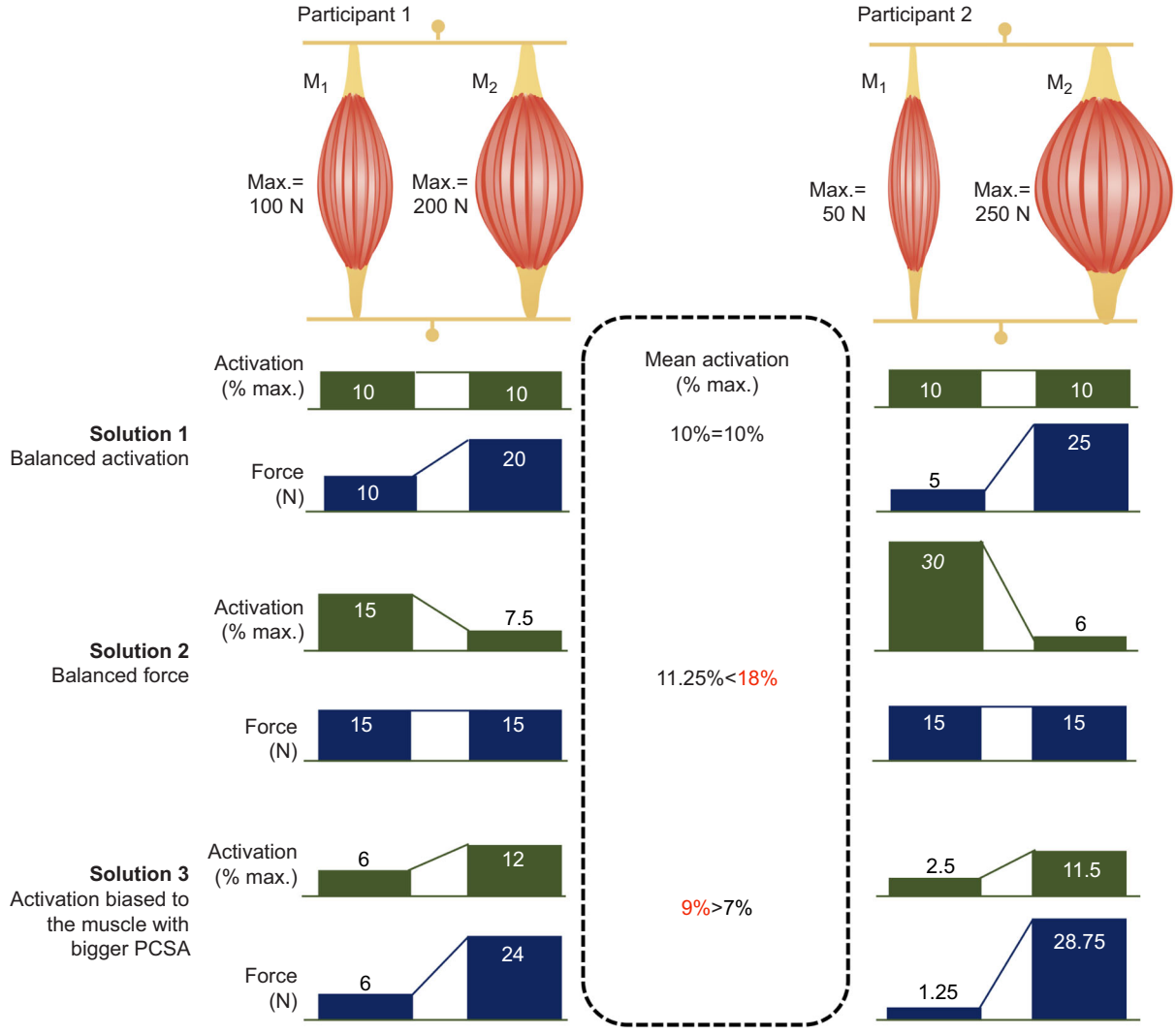

Fig. 1. Illustration to explain how the nervous system could account for individual differences in force-generating capacity between synergist muscles. M1 and M2 are two synergist muscles acting across the same joint(s). In the present case, M1 and M2 can be the gastrocnemius medialis and lateralis. Solution 1: activation is equally shared between synergist muscles, in which case the imbalance of force would match the imbalance of the force-generating capacity. Solution 2: the force-sharing strategy is similar among individuals with either balanced or imbalanced force between synergist muscles. In this latter case, the distribution of activation would vary between individuals. Solution 3: the muscle with the higher force-generating capacity receives greater activation, in which case the overall activation would be reduced but a large imbalance of force would exist. Note that there is a solution 4 (not shown) in which there is no specific coupling between activation and force-generating capacities.

biarticular muscles (GL and GM) and one monoarticular muscle (SOL), providing the opportunity to test whether a similar coupling between the distribution of activation and the distribution of force-generating capacity exists between synergist muscles with different functions.

The overall aim of this study was to determine the relationship between the ratio of activation measured during an isometric submaximal plantarflexion task and the ratio of force-generating capacity between the three heads of the triceps surae. The comparison of the GM and GL enables us to understand the activation distribution of two muscles having identical functions and very different force-generating capacities, while the comparison of SOL and both gastrocnemii (Gas) provides insight into the activation distribution of muscles with different functions. We tested two hypotheses: (1) a positive correlation between GM/Gas activation and GM/Gas PCSA would exist, demonstrating a coupling between the distribution of activation and the distribution of force-generating capacity for the GM and GL (solution 3, Fig. 1) but not for muscles with different functions (SOL and Gas), and (2) this coupling would contribute to reduce the overall activation of the triceps surae and the metabolic cost. Further, we described the inter-individual variability of the force-sharing strategies. Data are discussed in relation to possible mechanical effects on the Achilles tendon.

MATERIALS AND METHODS

Participants

The study was conducted with 20 healthy volunteers (age: 26 ±6 years, height: 173±11 cm, body mass: 64.3±12.4 kg; 10 males and 10 females). Participants had no history of lower leg pain that had limited function or required them to seek intervention from a healthcare professional within the past 6 months. Participants were informed of the methods used before providing written consent. The experimental procedures were approved by the local ethics committee (Rennes Ouest V, CPP-MIP-010) and all procedures adhered to the Declaration of Helsinki.

Protocol

Within a 2-month period, participants attended three sessions: one magnetic resonance imaging session, where images were taken and used to measure muscle volume and tendon moment arm (moment arm data not reported here); and two experimental sessions during which they performed a series of maximal and submaximal isometric plantarflexion tasks while muscle activation was recorded. The two experimental sessions were interspaced by at least 1 day, in order to test the between-day reliability of muscle activation strategies. Measurements of fascicle length and pennation angle needed for functional PCSA estimation were performed following the plantarflexion tasks, during one of the two experimental sessions.

During the experimental sessions, the participants performed isometric plantarflexion tasks lying prone (hip and knee fully extended) on a dynamometer (Con-Trex, CMV AG, Dübendorf, Switzerland). This knee position ensured a contribution of the three heads of the triceps surae to plantarflexion torque. The right foot was fixed to the dynamometer with inextensible straps. After a standardized warm-up, the participants performed five maximal isometric voluntary ankle plantarflexions [maximal voluntary contractions (MVCs)] for 3 s, with 120 s rest in between. Two out of the five MVCs were randomly chosen to test the voluntary activation level using the twitch interpolation technique. This procedure (described in detail below) aimed to determine whether the participants produced true maximal efforts. The submaximal tasks involved: (i) submaximal isometric torque-matched tasks set at 20% of MVC, and (ii) increasing isometric plantarflexion torque linearly from a relaxed state to 70% of MVC over a 10-s period. Each submaximal task was repeated four times (eight contractions in total) in a random order. Feedback of the torque output was displayed to the experimenter and the participant.

Estimation of muscle activation

Surface electromyography

Myoelectrical activity was collected from three muscles of the right leg: GM, GL and SOL. Skin was first shaved and cleaned with alcohol to minimize the skin–electrode impedance and facilitate electrode fixation. For each muscle, a pair of surface Ag/AgCl electrodes (diameter of the recording area: 5 mm; Kendall Medi-Trace^{TM}, Canada) was attached to the skin with a ~20 mm inter-electrode distance (centre-to-centre). Electrode location was checked with a B-mode ultrasound (v11.0, Aixplorer, Supersonic Imagine, Aix-en-Provence, France) to ensure that they were positioned away from the borders of the neighbouring muscles and aligned with fascicle direction. Electrode cables were well secured to the skin with adhesive tape to minimize movement artefacts. EMG signals were pre-amplified close to the electrodes and digitized at 1000 Hz using an EMG amplifier unit (ME6000, Mega Electronics Ltd, Finland).

Voluntary activation level

For each muscle, the EMG amplitude recorded during submaximal contractions was normalized to that measured during MVCs. It was therefore critical that each participant produced a true maximal contraction. To verify that the plantar flexors were maximally activated, a doublet electrical stimulus (inter-stimulus interval: 10 ms; duration of the stimulus: 1 ms; amplitude: 400 V) was delivered during two of the five MVCs, by a constant current stimulator (DS7AH, Digitimer, UK) through two electrodes. This was delivered to the tibial nerve using the self-adhesive cathode (50 mm diameter), placed over the nerve in the popliteal fossa, and the anode (80×130 mm), placed over the anterior tibial tuberosity. To determine the maximal amplitude of the resting twitch, the output current was incrementally increased (from 0 mA, with an incremental step of 5 mA) until a maximum ankle plantarflexion torque was reached despite an increase in current intensity. To ensure maximal response during testing, a supramaximal stimulus intensity of 120% of the intensity previously determined was used (mean: 127.5±38.6 mA). Participants were informed about the electrical stimulation just prior to these particular contractions. The supramaximal doublet stimulus was delivered during the plateau of the MVC, and within 5 s in the subsequent rest period to elicit superimposed and resting twitches, respectively.

Mechanical and electromyography data analysis

Force and EMG signals were processed using MATLAB (The MathWorks, Natick, MA, USA). Force signals were low-pass filtered at 10 Hz. Then, MVC torque was calculated from the maximal contractions performed without twitch interpolation as the maximal torque over a 300-ms moving average. The percentage of voluntary activation was measured from the torque signal according to the equation of Todd et al. (2004):

$$\text{Voluntary activation} = \left(1 - \frac{\text{Superimposed twitch}}{\text{Resting twitch}}\right) \times 100. \quad (1)$$

Raw EMG signals were first visually inspected for noise or artefact. Among the 440 trials [11 trials (3 MVCs+4 submaximal trials+4 ramp trials)×2 sessions×20 participants], 13 trials (8 submaximal tasks and 5 ramp trials) were excluded because of electrical noise confirmed by a fast Fourier transformation analysis. EMG results were averaged between the remaining trials such that there were no missing data in the statistics. The maximal root mean square EMG (EMG_{RMS}) was calculated from the MVCs performed without twitch interpolation as the maximal EMG_{RMS} value over a 300 ms time window. During the submaximal isometric force-matched tasks, the EMG_{RMS} was calculated over 5 s at the middle of the force plateau. During the ramp tasks, EMG_{RMS} was calculated over 300 ms time windows and linearly interpolated to a torque-scale ranged from 0% to 70% of MVC. For each muscle, these values were normalized to the maximal EMG_{RMS} measured during the MVC ($EMG_{RMS,max}$). The ratio of activation (%) was calculated from these normalized values as follows:

$$\frac{\text{Muscle } i}{\text{Triceps surae}} = \frac{EMG_{RMS,i}}{EMG_{RMS,GM} + EMG_{RMS,GL} + EMG_{RMS,SOL}} \times 100. \quad (2)$$

Note that the GM/Gas ratio (%) was also considered and calculated as follows:

$$\frac{GM}{Gas} = \frac{EMG_{RMS,GM}}{(EMG_{RMS,GM} + EMG_{RMS,GL})} \times 100. \quad (3)$$

Muscle physiological cross-sectional area

Because of the pennated structure of the three muscle heads, the whole component of the force developed by the fibres does not act in the line of action (Haxton, 1944). Therefore, the pennation angle was considered for functional PCSA calculation, as proposed in previous work (Lieber, 2002; Sacks and Roy, 1982). Functional PCSA was calculated as follows:

$$PCSA = \frac{V}{L_f} \times \cos(\theta_p), \quad (4)$$

where V is muscle volume in cm^3, L_f is fascicle length in cm and θ_p is pennation angle in deg. As for EMG (Eqns 2 and 3), the following ratios of PCSA were calculated: GM/Gas, GM/TS, GL/TS and SOL/TS.

Muscle volume

Volumetric acquisitions of the lower leg (from heel to mid-thigh) were performed using a 3T magnetic resonance imaging scanner (Ingenia, Phillips, The Netherlands) using a three-dimensional e-THRIVE sequence (repetition time: 6.0 ms, echo time: 3.0 ms, field of view: 400×400×199.5 mm, voxel size: 0.70×0.70×3.00 mm, flip angle: 10 deg). Slice thickness was 6 mm without an inter-slice gap. This sequence was chosen to enhance the separation between muscles. Two to three volumes were acquired to cover the whole lower leg, with the participants in supine position, lying with their hip and knee fully extended, and the foot held perpendicular to the shank. Magnetic resonance images were analysed using 3D image analysis software (Mimics, Materialise, Belgium). GM, GL and SOL were segmented manually on each slice by an experienced examiner, from the distal slice, where the SOL could first be visualized to the most proximal slice, where the GM and GL insertions were visible. As GL and SOL were fused in some slices within the proximal region, we used the visible landmarks on the preceding and subsequent images to assist the segmentation between muscles. A 3D reconstruction was performed (Mimics; option=optimal; Fig. 2) before the volume of each muscle was calculated.

Muscle fascicle length and pennation angle

An ultrasound scanner (Aixplorer v11.0, Supersonic Imagine, France) coupled with a 50 mm linear probe (4–15 MHz; SuperLinear 15-4, Vermon, Tours, France) was used in panoramic mode to assess the fascicle length of GM, GL and SOL muscles. This mode uses an algorithm that fits a series of images, allowing scanning of entire fascicles within one continuous scan (Hedrick, 2000). The advantage of this method over classical measurements from one B-mode image is that it does not require extrapolating the non-visible part of the fascicle, thus providing a more accurate estimation of muscle fascicle length (Noorkoiv et al., 2010).

To verify the accuracy of the in-built panoramic mode, we performed a pilot study on a bovine sample (approximately 30×10×5 cm). Four needles were inserted through the meat sample. The needle extremities remained visible outside the meat, and a retro-reflective marker (diameter: 10 mm) was attached to each needle extremity (a total of eight markers). The inter-needle distances were determined using an optoelectronic motion capture system composed of four cameras (Flex 13, Optitrack, Natural Point, USA). The inter-needle distances (from midline to midline) were 4.32, 4.85 and 6.75 cm; and the straight distance between the first and fourth needles was 15.16 cm. Three ultrasound panoramic scans were performed; the reliability of the inter-needle distance measured during these three trials was excellent (for all distances, CV<1.3%). The three trials were averaged, and then compared with the distances measured using the motion capture system, to test the accuracy of the measurement. The absolute error percentage was lower than 2.2%.

For the fascicle length and pennation angle measurement protocol, participants were placed in the same position as was used for the experimental tasks, i.e. lying prone, hip and knee fully extended, and the ankle maintained at 0 deg. The proximal and distal insertions and the medial and lateral borders of the GM and GL were located using B-mode ultrasound. A line was drawn on the skin at the middle of the muscle belly from the distal to the proximal insertion following the fascicle path. The US probe was then placed on the line and oriented within the plane of the fascicles. The scan consisted of moving the probe along this line with minimal pressure applied to the skin, to minimize compression of the muscle. Two reconstructed panoramic images were recorded per muscle (Fig. 3). To assess the SOL fascicle length and pennation angle, the US probe was placed over the GL myotendinous junction. This probe location was chosen because fascicles were clearly visible. Although the SOL has a multipennate structure, a recent study investigating the 3D architecture of the whole SOL muscle reported no difference in fascicle length between its four compartments (medial–anterior, lateral–anterior, medial–posterior and lateral–posterior) (Bolsterlee et al., 2018). We therefore considered that our probe location provided fascicle length data that were representative of the whole muscle. As SOL fascicle length was shorter than that of the GM and GL, entire fascicles were measured from two conventional B-mode ultrasound images. For each image, we aimed to measure three fascicles (proximal, mid distance and distal) leading to a total of up to six fascicles analysed per muscle and per operator. Owing to technical problems with some images, an average of 6, 5.5 and 3.9 fascicles were measured for the GM, GL and SOL, respectively. As some fascicles exhibited a small curvature, we used a segmented line with a spline fit to model the fascicles and calculate their length (Fig. 3; ImageJ V1.48, National Institutes of Health, Bethesda, MD,

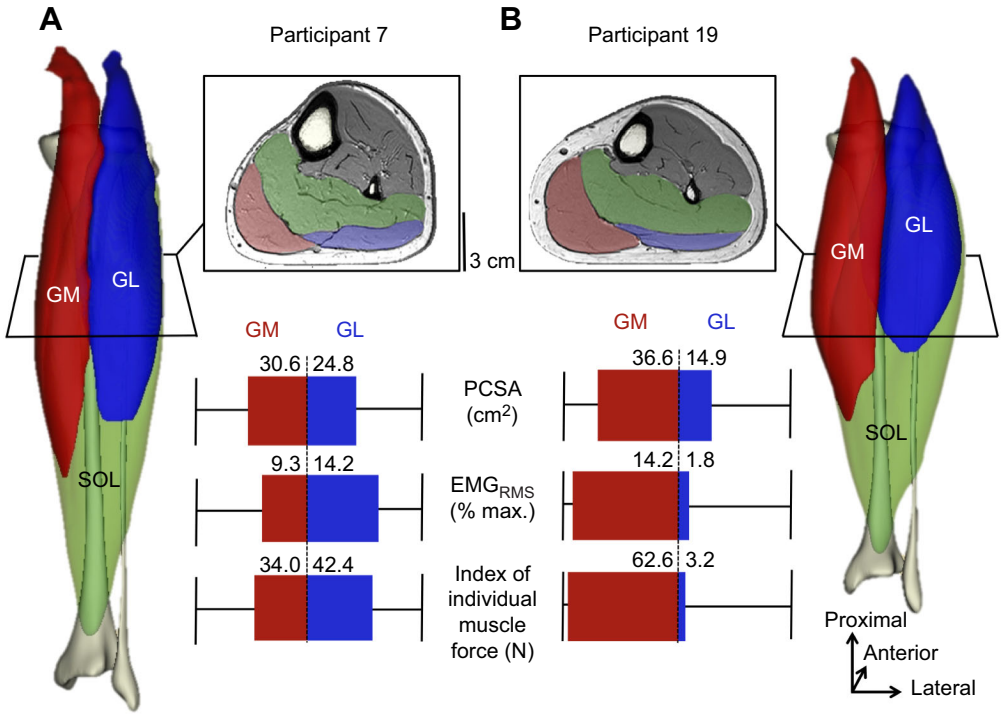

Fig. 2. Individual examples of data from two participants. Each muscle was manually segmented from each axial image, as depicted in the middle-top of th figure. The gastrocnemius medialis [GM (red)], gastrocnemius lateralis [GL (blue)] and soleus [SOL (green)] are shown. Example axial slices are from ~33% of th proximo-distal part of the leg. Muscle volumes were reconstructed in 3D (lateral panels). Then, measures of muscle balance were calculated (middle-bottom panel). (1) Functional physiological cross-sectional area (PCSA) was calculated from muscle volume, fascicle length and pennation angle (measured using panoramic ultrasound images, see Fig. 3). (2) Muscle activation was measured during a submaximal isometric plantarflexion task performed at 20% of the maximal voluntary contraction (EMG_{RMS}; % max.). (3) The index of individual muscle force was calculated by multiplying PCSA, muscle activation and specifi tension (based on theoretic values; see Materials and Methods). In the examples here, the GM/Gas index of force was 44.5% for participant 7 (A) and 95.1% fc participant 19 (B), which highlights an extreme difference between participants.

USA). The pennation angle was calculated as the angle between the fascicles and the deep aponeurosis of the muscle. Values were then averaged across fascicles within a muscle to obtain a representative fascicle length and pennation angle of the whole muscle.

Estimation of an index of metabolic cost

As indicated above, muscle force is proportional to the PCSA of active muscle fibres. Therefore, muscles with long fibres require a larger active muscle volume to generate a given force (Biewener, 2016). As such, they consume more ATP per unit force generated than muscles with short fibres. In this way, an index of overall metabolic cost was calculated by considering active muscle PCSA and muscle volume of muscle i, as follows:

$$\text{Index of metabolic cost} = \sum_{i=1}^{3} \frac{\text{PCSA}_i \times \text{EMG}_{\text{RMS},i}}{V_i}, \quad (5)$$

where muscles 1 to 3 are the GM, GL and SOL, respectively.

Estimation of an index of individual muscle force

Even though individual muscle force can be measured in freel moving animals using force transducers placed on each subtendo (Herzog et al., 1993; Walmsley et al., 1978), this invasive techniqu cannot be used in humans. The force produced by a muscle depend on both the activation it receives and several biomechanical factor such as its PCSA, force–length and force–velocity relationship and specific tension (P_0). Because the force–length and force velocity relationships remain challenging to estimate *in vivo*, w focused on isometric contractions during which we considered tha these relationships played a minor role in the difference of forc produced by the synergist muscles. In other words, we considere that the difference of force between the synergist muscles depende mainly on their PCSA, their activation and their specific tensio Therefore, an index of muscle force (N) was calculated for the 20% hold contraction as follows:

$$\text{Index of force} = \text{PCSA} \times \text{EMG}_{\text{RMS,normalized}} \times P_0, \quad (6$$

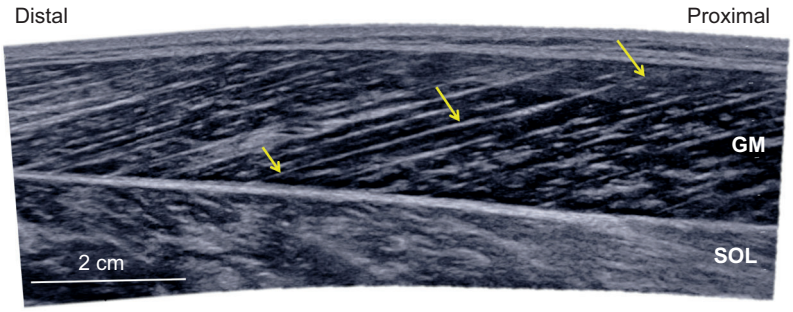

Fig. 3. Individual example of a panoramic ultrasound image for the gastrocnemius medialis (GM) muscle. This image was used to calculate GM fascicle length. The yellow arrows indicate a fascicle. SOL, soleus.

where EMG_{RMS} is expressed as a percentage of the $EMG_{RMS,max}$, PCSA in cm^2 and specific tension in N cm^{-2}. Given the size principle of orderly recruitment (Henneman and Oslon, 1965; Henneman et al., 1965), it is likely that small motor units were preferentially recruited at 20% of MVC. As each head of the triceps surae is composed by more than 20% of slow fibres (50.8, 46.9 and 87.7% for GM, GL and SOL, respectively) (Johnson et al., 1973), we reasonably assumed that only slow fibres were active. We therefore considered values of specific tension reported for slow fibres, i.e. 12 N cm^{-2} (Fitts et al., 1989; Larsson and Moss, 1993). As for EMG and PCSA, the following ratios of force index were calculated: GM/Gas, GM/TS, GL/TS and SOL/TS.

Statistics

Statistical analyses were performed in Statistica v7.0 (Statsoft, Tulsa, OK, USA). Distributions consistently passed the Shapiro–Wilk normality test and all data are reported as means±s.d. To test the robustness of the activation strategies, the between-day reliability of the EMG data was tested using the intra-class correlation coefficient (ICC) and the standard error of measurement (s.e.m.).

Separate repeated-measures ANOVAs were used to determine whether volume, fascicle length, functional PCSA and the PCSA/volume ratio were different between muscles [within-subject factor: muscle (GM, GL and SOL)]. Ratios of muscle activation and ratios of muscle force estimated during the submaximal tasks at 20% of MVC were compared separately with a repeated-measures ANOVA [within-subject factor: ratio (GM/Gas, GM/TS, GL/TS and SOL/TS)]. To test the effect of contraction intensity on the ratio of muscle activation, we performed a repeated-measures ANOVA for each ratio of activation separately (GM/Gas, GM/TS, GL/TS and SOL/TS) [within-subject factor: torque (every 10% from 10 to 70% of MVC)]. When appropriate, *post hoc* analyses were performed using the Bonferroni test.

To test the first hypothesis, we determined the relationship between the ratio of activation and the ratio of PCSA using Pearson's correlation coefficient. We only considered the GM/Gas and the SOL/TS ratios to understand the neuromechanical coupling of two muscles having identical (GM and GL) or different (SOL and Gas) functions. Note that the correlation made with GM/TS and GL/TS ratios would have contained redundant information with the other two ratios. To test the second hypothesis, we used Pearson's correlation coefficient to assess the relationship between ratios of activation and either the normalized EMG amplitude averaged across the three muscles or the index of metabolic cost. The level of significance was set at $P<0.05$.

RESULTS

Muscle activation

Voluntary activation level

The maximal isometric plantarflexion torque measured during the contractions performed without twitch interpolation was 124.0±28.8 Nm. Participants reached a voluntary activation level of 98.4±3.3% (range: 92.1–100%) and 99.1±2.4% (range 95.0–100%) during the first and second sessions, respectively. As such, we considered that the maximal EMG_{RMS} measured during the MVC tasks represented the maximal activation for all of the studied muscles.

Isometric contractions at 20% of MVC

The between-day reliability of the normalized EMG_{RMS} values was excellent (ICC>0.81, SEM<2.8% of $EMG_{RMS,max}$; Table 1). Reliability of the ratio of activation was good to excellent (ICC>0.71, s.e.m.<6.8%; Table 1). Overall, this provides evidence that the coordination strategies were robust between days. Thus, EMG data were averaged between the two sessions for further analysis.

Table 1. Between-day reliability of muscle activation (EMG_{RMS}) and activation ratios measured during the submaximal isometric force-matched tasks at 20% of maximal voluntary contraction (MVC)

	Muscle activation			Activation ratios			
	GM	GL	SOL	GM/Gas	GM/TS	GL/TS	SOL/TS
ICC	0.83	0.84	0.81	0.80	0.81	0.76	0.71
s.e.m. (%)	2.0	1.3	2.8	6.8	5.6	3.5	5.4

ICC, Intra-class coefficient of correlation; s.e.m., standard error of measurement (expressed in % of $EMG_{RMS,max}$ for EMG_{RMS} values and as % for the ratios); GM, gastrocnemius medialis; GL, gastrocnemius lateralis; SOL, soleus; TS, triceps surae. n=20.

The activation ratios during the isometric 20% MVC contractions were: GM/Gas, 65.0±13.2% (range: 37.7–88.7%); GM/TS, 36.3±11.4% (range: 19.1–57.0%); GL/TS, 18.8±6.4% (range: 7.3–31.6%); and SOL/TS, 44.8±8.9% (range: 26.4–61.0%). The GL/TS ratio was lower than both the GM/TS ratio ($P<0.001$) and the SOL/TS ratio ($P<0.001$); there was no difference between the GM/TS and SOL/TS ratios despite the P-value being close to significance ($P=0.06$). Notably, there was a large variability between individuals (Fig. 4).

Isometric ramp contractions

There was a main effect of torque level on both the GL/TS ($P<0.001$) and SOL/TS ($P<0.001$) ratios of activation (Fig. 5). Specifically, the GL/TS ratio measured at 10% of MVC was significantly lower than that measured at 40% of MVC and above (all $P<0.01$). In other words, the relative contribution of the GL increased with contraction intensity. Also, the SOL/TS ratio measured at 10% of MVC was significantly higher than that measured at 50% of MVC and above (all $P<0.02$). This indicates that the contribution of SOL relative to the whole triceps surae decreased with contraction intensity. Together, these results provide evidence that the contribution of GL and SOL tend to be closer to 33% (i.e. balanced activation between the three muscles) as contraction intensity increased. Note that the GM/TS ratio of activation was not affected by contraction intensity (main effect of torque level: $P=0.97$), and contributed ∼33% of the total triceps surae activation throughout the ramp contraction.

Physiological cross-sectional area

There was a main effect of muscle ($P<0.001$) on volume, with SOL volume being systematically larger than that of GM ($P<0.001$) and GL ($P<0.001$). GM volume was also larger than that of GL ($P<0.001$; Table 2). There was a main effect of muscle ($P<0.001$) on fascicle length. Specifically, SOL exhibited a shorter fascicle length than both GM ($P<0.001$) and GL ($P<0.001$). Further, GM fascicle length was shorter than GL fascicle length ($P<0.001$; Table 2). There was a main effect of muscle ($P<0.001$) on pennation angle. Specifically, GL had a smaller pennation angle than both GM ($P<0.001$) and SOL ($P<0.001$). There was no difference between GM and SOL.

Consistent with volume and fascicle length differences, there was a main effect of muscle ($P<0.001$) on functional PCSA (Table 2). SOL PCSA was systematically larger than GM ($P<0.001$) and GL PCSA ($P<0.001$), and GM PCSA was larger than GL PCSA ($P<0.001$). The ratio of PCSA was 68.6±4.6% (range 55.2–74.0%) for GM/Gas, 27.2±4.0% (range 17.9–33.1%) for GM/TS,

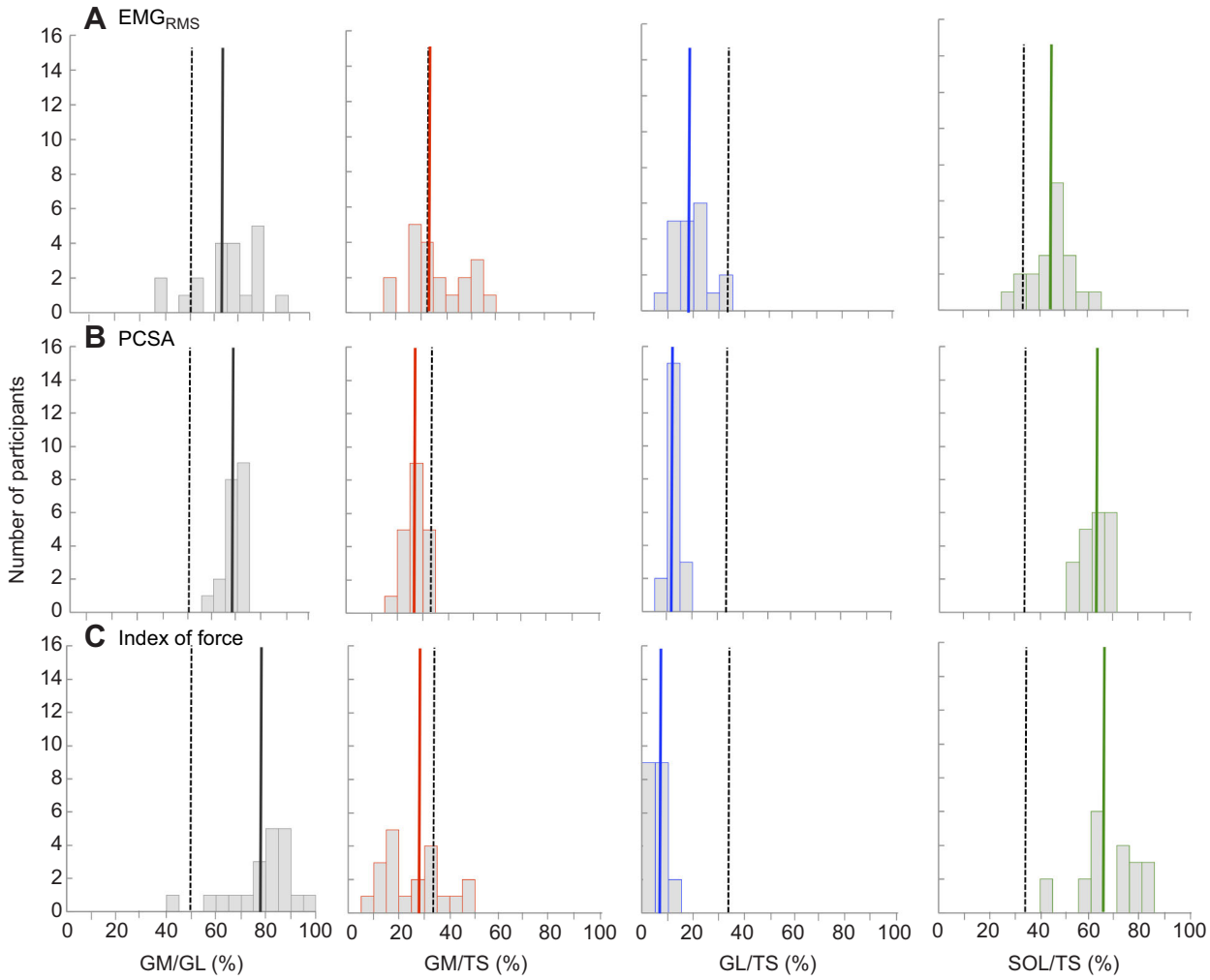

Fig. 4. Group distribution of (A) the ratio of activation (EMG_{RMS}), (B) the ratio of physiological cross-sectional area (PCSA) and (C) the ratio of index of force. Results are from the submaximal contraction performed at 20% of the maximal voluntary contraction. Vertical bold lines depict the mean results reported in the present study, and the dashed lines depict what would be a balanced ratio between synergist muscles (i.e. 50% for GM/Gas and 33.3% for ratios with three muscles considered). GM, gastrocnemius medialis; GL, gastrocnemius lateralis; SOL, soleus. TS, triceps surae. *n*=20.

12.4±2.4% (range 8.8–19.5%) for GL/TS and 60.4±5.2% (range 50.6–68.5%) for SOL/TS. The variability between participants was large (Fig. 5).

Relationship between activation and muscle PCSA

There was a significant positive correlation (r=0.53, P<0.005) between the ratio of GM/Gas activation measured during the force-matched task at 20% of MVC and the ratio of GM/Gas PCSA (Table 3). This indicates that the greater the force-generating capacity of GM compared with GL, the stronger bias of activation to the GM. Significant positive correlations were also observed when considering this activation ratio measured during the ramp contraction at intensities between 10 and 50% of MVC (0.51<r<0.62, all P<0.025; Table 3). No significant correlation was observed at 60 and 70% of MVC when the ratio of GM/Gas activation tended toward 50%. When considering the SOL/TS ratios (activation versus PCSA), there was no significant correlation (all r<0.33, all P>0.05; Table 3).

Consequences of the neuromechanical coupling on overall activation and metabolic cost

To interpret the consequences of the coupling between the ratio of GM/Gas activation and the ratio of GM/Gas PCSA, we first explored the relationship between the ratio of GM/Gas activation and the normalized EMG amplitude averaged across the three muscle heads. We observed a negative significant correlation at 30% of MVC and above (–0.66<r<–0.42, P<0.05; Table 4, Fig. 6). This confirms the hypothesis that the coupling between the distribution of PCSA and the distribution of activation contributes to a reduction of the overall activation of the triceps surae. Interestingly, slightly larger correlations were observed when considering the index of metabolic cost (–0.74<r<–0.52, P<0.05; Table 4, Fig. 6). Fig. 6 depicts a 3D representation of the relationship between GM/Gas activation, contraction intensity and either mean activation [R^2 (linear fit)=0.94; Fig. 6A] or the index of metabolic cost [R^2 (linear fit)=0.93; Fig. 6B]. Note that no significant correlation was observed when considering the ratio of SOL/TS activation (all r<–0.41 for correlations with activation and all r< 0.39 for correlations with the index of metabolic cost).

Inter-individual variability of force-sharing strategies

For the sake of clarity, indexes of force are reported only for the submaximal contraction performed at 20% of MVC. Using Eqn 6, indices of force were 69.0±37.1, 17.3±11.0 and 200.5±103.1 N for the GM, GL and SOL, respectively. The mean ratio of force index was 78.9±12.6%, 26.2±11.8%, 6.0±2.5% and 67.8±11.6% for

Journal of Experimental Biology (2018) 221, jeb187260. doi:10.1242/jeb.187260

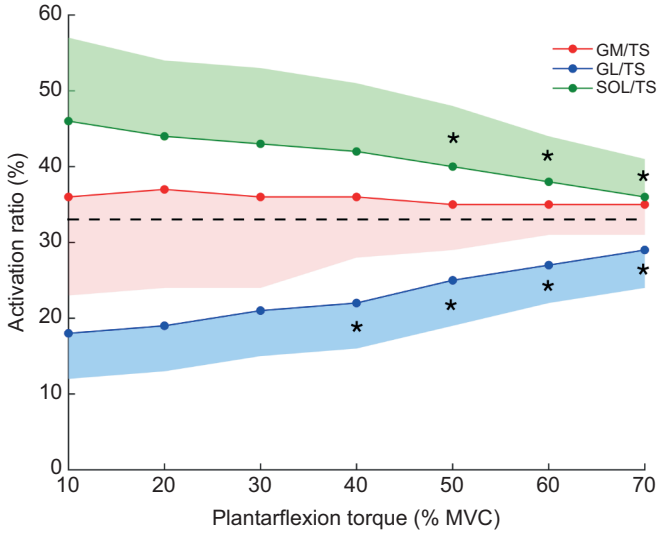

Fig. 5. Ratios of muscle activation as a function of contraction intensity. GM/TS (red), GL/TS (blue) and SOL/TS (green) logically converge to 33% (balanced activation) as contraction intensity increased. MVC, maximal voluntary contraction; GM, gastrocnemius medialis; GL, gastrocnemius lateralis; SOL, soleus; TS, triceps surae. * indicates significant difference compared with 10% of MVC. *n*=20.

GM/Gas, GM/TS, GL/TS and SOL/TS, respectively. The GL/TS force ratio was significantly lower than that for GM/TS ($P<0.001$) and SOL/TS ($P<0.001$). The GM/TS force ratio was significantly lower than that for SOL/TS ($P<0.001$). Very large variability between individuals is highlighted in Fig. 4.

DISCUSSION

This study has several novel findings. First, although there was no significant correlation between the distribution of activation and the distribution of force-generating capacity between monoarticular and biarticular muscles (SOL/TS ratio), a positive correlation was observed when considering the two biarticular muscles that share the same function (GM/Gas ratio). Specifically, the greater the force-generating capacity of the GM compared with the GL, the stronger bias of activation to the GM. Second, a higher ratio of GM/Gas activation was associated with lower triceps surae activation and metabolic cost. Third, there was a significant force imbalance between synergist muscles, the magnitude of which varied greatly between participants. These results provide insight into our understanding of the interplay between the activation a muscle receives and its torque-generating capacity. Also, these observations may have clinical relevance as they provide the impetus to consider individual muscle coordination strategies as an intrinsic risk factor to the development of Achilles tendinopathy.

Distribution of muscle activation

Because of its important role during balance and locomotion, the triceps surae has received much attention in the literature. In the studies that focused on muscle activation, GM and GL muscles are often considered equivalent such that only the GM (Duysens et al., 1991) or GL (Kyrolainen and Komi, 1994) is measured. Further, biomechanical models often consider the GL and GM as a single muscle (Herzog et al., 1991; Winter and Challis, 2008). However, multiple studies provide evidence that activation is not balanced between these muscles, with the vast majority of studies reporting higher activation for the GM than the GL during a wide variety of tasks, e.g. standing (Héroux et al., 2014), calf raises (Fiebert et al., 2000; Riemann et al., 2011) and submaximal isometric plantarflexion (Cresswell et al., 1995; Lacourpaille et al., 2017; McLean and Goudy, 2004). All these results are in line with our results showing on average a two times higher activation of the GM than the GL during the isometric plantarflexion at 20% of MVC. In the present study, the SOL exhibited a slightly greater activation level than both the GM and GL, which is consistent with results from Mademli and Arampatzis (2005), but inconsistent with those of Cresswell et al. (1995) and Masood et al. (2014), all being performed during isometric submaximal tasks but in varying positions. Note that an activation biased toward the SOL muscle, which exhibits both the biggest PCSA and the highest slow-twitch fibre content, may reduce the metabolic cost of the contraction at low contraction intensity, as discussed below. Logically, the imbalance of activation across the GM, GL and SOL tends to disappear at higher contraction levels (70% of MVC during the ramped contraction; Fig. 5), where near-complete activation of all synergists is required. It is important to note that the aforementioned results are derived from group data that are not representative of each individual.

The vast majority of studies on muscle coordination report values averaged from a group of individuals, making it impossible to appreciate the individual differences in the activation strategies that inevitably exist. Here, we report a wide range of activation ratio during a standardized isometric single-joint task. For example, during the 20% of MVC hold contraction, SOL/TS and GM/Gas activation ratios ranged from 26.4% to 61.0% and from 37.7% to 88.7%, respectively. To the best of our knowledge, this inter-individual variability has received little attention. During gait, Ahn et al. (2011) reported large differences in the ratio of activation between the GM and GL, with seven out of the 10 participants activating their GM more than their GL, and the other three

Table 2. Muscle architecture

	GM			GL			SOL		
	Males	Females	Mean	Males	Females	Mean	Males	Females	Mean
Volume (cm^3)	280.7±48.5	218.7±40.6	249.7±53.9*	171.2±22.9	104.2±20.4	137.7±40.3‡	489.4±75.5	350.9±60.8	420.1±97.5*,‡
FL (cm)	5.1±0.8	5.8±0.7	5.4±0.8*	6.2±0.5	6.7±0.9	6.4±0.7‡	3.6±0.9	4.2±0.6	3.9±0.8*,‡
PA (deg)	21.6±3.8	17.3±1.7	19.5±3.6*	13.2±2.7	9.1±1.9	11.2±3.1‡	24.4±7.0	16.3±3.8	20.3±6.9*
PCSA (cm^2)	54.7±11.7	37.5±5.3	46.1±13.2*	27.0±3.3	15.5±2.9	21.3±6.6‡	127.9±25.4	80.3±14.3	104.1±31.6*,‡
PCSA/volume (10^3 cm^{-1})	19.5±3.0	17.4±2.2	18.5±2.8*	15.8±1.2	15.1±1.9	15.5±1.6‡	26.3±4.5	23.1±2.8	24.7±4.0*,‡

Volume, fascicle length (FL), pennation angle (PA), physiological cross-sectional area (PCSA) and the ratio PCSA/volume are reported for males and females separately to facilitate comparison with other works. Statistics are only reported for mean values; *n*=20. GM, gastrocnemius medialis; GL, gastrocnemius lateralis; SOL, soleus.

*Indicates significant difference with GL.

‡Indicates significant difference with GM.

Journal of Experimental Biology (2018) 221, jeb187260. doi:10.1242/jeb.187260

Table 3. Correlation coefficients between the ratio of EMG_{RMS} and the ratio of physiological cross-sectional area (PCSA)

	Activation ratios	
% MVC	GM/Gas	SOL/TS
10	0.59*	0.10
20 hold	0.53*	0.34
20	0.62*	0.11
30	0.61*	0.11
40	0.60*	0.03
50	0.51*	−0.03
60	0.34	−0.26
70	0.20	−0.25

MVC, maximal voluntary contraction; GM, gastrocnemius medialis; GL, gastrocnemius lateralis; SOL, soleus; TS, triceps surae. 20 hold represents the results obtained during the isometric contractions performed separately at 20% of MVC.
*Indicates a significant correlation (P<0.05). n=20.

Table 4. Correlation coefficients between the ratio of EMG_{RMS} and both the mean activation of the triceps surae and the index of overall metabolic cost

% MVC	GM/Gas EMG versus mean TS activation	GM/Gas EMG versus overall metabolic cost
10	−0.12	−0.21
20 hold	−0.21	−0.37
20	−0.30	−0.38
30	−0.42*	−0.52*
40	−0.56*	−0.62*
50	−0.55*	−0.65*
60	−0.59*	−0.74*
70	−0.66*	−0.68*

The ratios of EMG_{RMS} were estimated during the submaximal isometric tasks isometric performed at 20% (20 hold) of the maximal voluntary contraction (MVC) and from 0 to 70% of MVC. Indices of overall metabolic cost were calculated by considering active muscle PCSA and muscle volume. TS, triceps surae.
*Indicates a significant correlation (P<0.05). n=20.

participants activating their GM and GL nearly equally. However, interpretation of the individual differences during gait requires considerations. Because body weight may influence the contraction intensity of the calf muscles during gait and because we report that activation ratios are affected by even small changes in contraction intensity (Fig. 5), it is difficult to determine whether the variability of activation ratios observed during gait is explained by different mechanical demand related to different body weights and/or by actual differences in activation strategies. Activation ratios between the heads of the triceps surae measured during a standardized isometric task have been reported in two previous studies (Masood et al., 2014; McLean and Goudy, 2004). Their results are in line with our observation that large individual differences in activation strategies exist. The novelty of our study among others is to demonstrate the robustness of these activation ratios across time, allowing us to consider that they represent individual-specific strategies. Another novelty of this study is to consider the relationship with the force-generating capacities, and therefore the mechanical consequence of these individual strategies.

Coupling between muscle activation and PCSA

In this study, we considered both muscle activation and functional PCSA to interpret the mechanical consequences of individual differences in muscle activation. The SOL exhibited a much larger PCSA than both the GM (×2.6) and the GL (×5.5). This large PCSA imbalance was a prerequisite for the present study, which aimed to assess the mechanical coupling within a group of synergist muscles with large difference in PCSA. Overall, the PCSA and volume values we estimated are very close to those reported by Albracht et al. (2008) and Fukunaga et al. (1996), respectively. Inspection of data for individual participants revealed large variability of the PCSA distribution among the three heads of the triceps surae, albeit with smaller magnitude than that observed for activation. For example, the GM/Gas and SOL/TS PCSA ratios ranged from 55.2% to 74.0% and from 50.6% to 68.5%, respectively. To our knowledge, this is the first study to report such individual differences for this muscle group.

Our first aim was to determine the nature of the relationship between the ratio of activation and the ratio of functional PCSA (considered as force-generating capacity). We observed a positive correlation between GM/Gas activation and GM/Gas PCSA, indicating that the greater the force-generating capacity of the GM compared with the GL, the stronger bias of activation to the GM. This was observed for the 20% hold plantarflexion and during the ramp contraction from 10 to 50% of MVC (Table 3). This result is in line with previous findings (Hug et al., 2015), showing a similar correlation when considering the lateral and medial heads of the quadriceps.

In the present study, we also considered synergist muscles that share different functions, i.e. monoarticular for SOL and biarticular for GM and GL. When considering data averaged over the whole population, the ratio of SOL/TS activation was higher than both GM/TS and GL/TS activation ratios at low contraction intensities (Fig. 5). This strategy seems particularly economic considering that SOL exhibits the larger PCSA (Table 2) and the larger proportion of type I fibres (Johnson et al., 1973). In addition, its architecture with short fascicles (Table 2) leads to a lower metabolic cost per unit force. Indeed, for two muscles that are both producing the same force, that have the same volume and typology, but different fibre lengths (and PCSA), the muscle with the longer fibre lengths has a greater metabolic cost (for a review, see Biewener, 2016). However, this association between muscle activation and muscle architecture observed at the group level, from averaged data, could not explain the inter-individual variability in activation strategies. Indeed, we found no correlation between SOL/TS ratio activation and SOL/TS force-generating capacity at any of the contraction intensities. For the sake of clarity, we did not report the results for the SOL/GM and SOL/GL ratios, but it is important to note that considering these ratios did not change the outcome, i.e. there was no significant correlation between distribution of activation and distribution of PCSA ($-0.20<r<0.31$). Although we cannot rule out that this absence of significant correlation is explained by methodological considerations, as discussed below, we believe that difference in function between the SOL and the gastrocnemii might explain this result. Indeed, activation of biarticular muscles depends on moment demands at two joints (Prilutsky, 2000), making it complicated to comply at the same time with neuromechanical coupling and the constraints of the task. In other words, the distribution of activation between the monoarticular SOL muscle and the biarticular gastrocnemii muscles cannot be only determined by the difference of force-generating capacity between the SOL and the gastrocnemii, but also need to consider the task constraints, which depend on actions at both the ankle and knee joints. This is in accordance with previous results showing a partial uncoupling of SOL and gastrocnemii activity in response to altered torque and velocity during pedalling in humans (Wakeling and Horn, 2009), during paw shakes in cats (Smith et al., 1980) or during locomotion in cats

Journal of Experimental Biology (2018) 221, jeb187260. doi:10.1242/jeb.187260

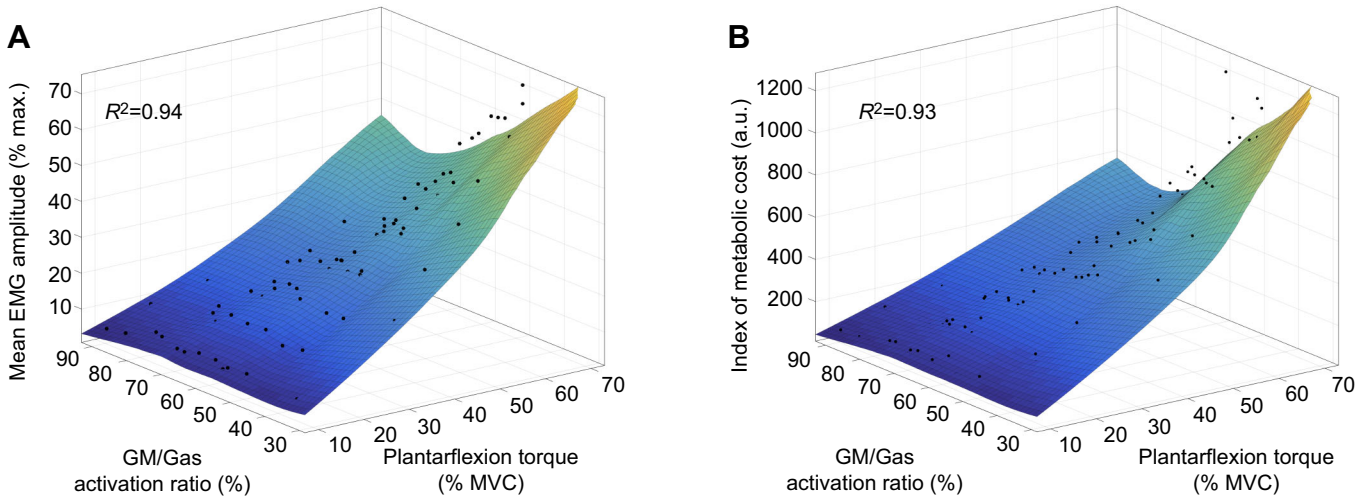

Fig. 6. Three-dimensional representation of the relationship between GM/Gas activation, contraction intensity and relationship between either (A) mean activation or (B) the index of metabolic cost. *n*=20.

(Walmsley et al., 1978). In the latter study, SOL force remained constant across speeds (from 0.6 to 3.0 m s^{-1}) while GM force increased with speed. As hypothesized for respiratory muscles (De Troyer et al., 2005), the distribution of muscle PCSA would be optimized to muscle function. As such, for muscles with multiple functions, PCSA might be optimized more for one function than another. The GM and GL muscles, involved in both plantarflexion and knee flexion, might have their PCSA set to knee flexion, such that knee flexion torque is maximized, while SOL might have its PCSA set to plantarflexion.

The absence of correlation when considering the distribution of activation and the distribution of PCSA between the SOL and the gastrocnemii might also be explained by the large difference in force-generating capacity, especially between the SOL and the GL. In the case of a positive coupling between activation and PCSA, large imbalances of force would be produced between these synergist muscles. These imbalances could ultimately have negative consequences for the Achilles tendon.

Benefits of the coupling between GM/Gas activation and GM/Gas PCSA

As presented in Fig. 1, a positive correlation between the distribution of force-generating capacity and the distribution of activation should lead to an overall lower activation, and thus a lower effort. This was partially confirmed by the negative correlation between the ratio of GM/Gas activation and the averaged normalized EMG amplitude observed during the ramp contraction at 30% of MVC and above (Table 4, Fig. 6). The lack of correlation at lower intensities (10 and 20% of MVC) could be explained by the contribution of other non-recorded plantarflexor muscles, which might have a greater relative contribution at these low intensities. For example, even though the participants were instructed to avoid compensatory strategies to produce plantarflexion torque, it remains possible that they used toe flexion at low intensities. Finally, it is also possible that the lack of significant correlation is explained by the relatively small sample size.

Similar results, with slightly larger coefficients of correlation (Table 4), were obtained when considering an overall index of metabolic cost calculated from the ratio PCSA/muscle volume and the relative muscle activation (Eqn 5). Because this index does not consider important parameters such as muscle typology, it represents only a crude estimate of metabolic cost. Despite this, we believe that the significant correlation between this index and the ratio of GM/Gas activation provides preliminary evidence that the GM/Gas activation strategy contributes to reduce the overall metabolic cost of the task.

It is important to note that in the triceps surae configuration, the muscle with the shortest fascicle length (SOL) is also the one with the biggest volume, and that the muscle with the longest fascicle length has the smallest volume (GL). This naturally results in the best combination to produce force: the muscle capable of producing the highest amount of force (with the biggest PCSA) is also the one with the most economic metabolic cost (smallest PCSA/volume ratio because of its smallest fascicle length; for a review, see Biewener, 2016). This can, at least in part, explain the relationship between the index of metabolic cost and the ratio of GM/Gas activation, and the higher ratio of SOL/TS activation observed at the group level.

Overall, these results align particularly well with theoretical models (Crowninshield and Brand, 1981; Dul et al., 1984). For example, Crowninshield and Brand (1981) proposed that individual muscle forces are selected such that the sum of muscle stresses cubed is minimized. Considering the linear relationship often reported between EMG amplitude and muscle force during isometric contractions, it is reasonable to consider that the mean activation that we calculated represents an index of the mean muscle stress. If we considered the cubed sum of normalized EMG amplitude instead of the sum, similar negative correlations with the ratio of GM/Gas activation were observed. Even though the model proposed by Crowninshield and Brand (1981) also predicted a positive correlation between SOL/TS PCSA and SOL/TS stress (or EMG), this was not confirmed by our experimental study. Another model proposed by Dul et al. (1984) considered that force-sharing strategy is chosen such that fatigue is minimized. Their model included information about the fibre type content in addition of muscle force-generating capacity. This approach echoes fairly well with the greater SOL/TS activation ratio observed at low intensity at the group level. In the absence of measurements of muscle fibre content, it is impossible to determine whether the model proposed by Dul et al. (1984) would predict well the wide range of individual strategies that we observed. Although these models may be relevant for well-controlled isometric tasks, it is important to acknowledge

that results obtained from direct measurement of muscle force during dynamic tasks in animals did not fit adequately with predictions made with the aforementioned models (Herzog and Leonard, 1991). Indeed, none of these models can predict the change in force-sharing observed with changes in the mechanical constraints of the task (GL and SOL in the cat: Herzog and Leonard, 1991; GM and SOL in the cat: Walmsley et al., 1978; GM and SOL in the cat: Whiting et al., 1984).

Individual force-sharing strategies and their functional consequences

These results have important implication for the understanding of individual force-sharing strategies. Importantly, for the force to be balanced across the three heads of the triceps surae, the muscle(s) with the lower force-generating capacity should be driven more. However, such a negative correlation was not observed, either for SOL/TS or GM/Gas. This finding provides evidence of an imbalance of force between the three heads, which varies considerably between participants (Fig. 4). Even though the inter-individual variability of force-sharing strategies has received little attention in the literature, such a large inter-individual variability can be inferred from experimental data measured in animals using force transducers. For example, the ratio of gastrocnemius/SOL peak force measured in five cats during downhill walking varied between 41.5% and 61.0% (data calculated from table 2 in Herzog et al., 1993). This force imbalance might have an important mechanical effect on the distal tendon (Achilles tendon) that is composed of three compartments, or fascicle bundles, that originate from each of the three heads of the triceps surae (Cummins and Anson, 1946; Szaro et al., 2009). The load distribution between Achilles subtendons is likely to be determined, at least in part, by the individual force-sharing strategy (Arndt et al., 1998; Bojsen-Møller and Magnusson, 2015; Kinugasa et al., 2013), with some strategies having the potential to induce suboptimal loading. For example, a direct relationship between individual muscle contributions and force distribution across the Achilles tendon has been demonstrated on cadaver preparations (Arndt et al., 1999).

Despite it being tempting to conclude that the large individual differences in force-sharing strategies that we report directly translate to individual differences in Achilles subtendon loading, intermuscular force transmission between the heads of the triceps surae may result in a redistribution of force between the Achilles subtendons, as recently suggested (Maas and Finni, 2018). It is also possible that every subtendon exhibits different mechanical properties (related to their elastic modulus, cross-sectional area, length) and that these properties vary between individuals. As such an imbalance of muscle force would not directly impose an imbalance of strain distribution between the subtendons. In this way, recent studies performed in rats (Finni et al., 2017) and humans (Pekala et al., 2017) have highlighted different mechanical properties between the three subtendons, with large differences between individuals (Pekala et al., 2017). Finally, the twisted structure of the Achilles tendon might also participate in reducing differences in strains between the subtendons (Edama et al., 2015).

As proposed in the literature, the distribution of loads and strains within the Achilles tendon could be involved in the development of Achilles pathology such as tendinopathy (Bojsen-Møller and Magnusson, 2015; Kannus, 1997). The present study provides evidence for individual-specific force-sharing strategies. Although it is possible that a subgroup of individuals exhibiting a specific profile of force-sharing strategy is more at risk of developing Achilles tendinopathy, it remains to be demonstrated.

Methodological considerations

There are multiple methodological limitations that require consideration. First, muscle activation was indirectly assessed using surface EMG. In order to minimize crosstalk and to ensure similar electrode location between participants, we used a standardized procedure. Specifically, we determined anatomical landmarks and we used B-mode ultrasound to check the appropriate location of the surface electrodes, away from the border of neighbouring muscles. Despite these precautions, we cannot exclude the possibility that part of the individual differences in EMG amplitudes may originate from slightly different placement of the electrodes relative to an individual's anatomy. However, the good between-day reliability of the EMG data (Table 1) provides some evidence that small changes in electrode location did not significantly alter the results. Second, for between-muscle and between-participant comparisons, it was important to normalize the RMS EMG values measured during the submaximal tasks to those measured during MVC. For this normalization procedure to be correct, we ensured that participants reached the maximal voluntary activation level during the MVC task. Results showing voluntary activation close to 100% make us confident that the normalization procedure was appropriate. Third, we focused on an isometric task because between-muscle difference in torque-generating capacity during a dynamic task requires knowledge of various mechanical factors that are difficult to estimate for each individual *in vivo* (e.g. force–velocity and force–length relationships, change in moment arm as a function of joint angles). We therefore considered the differences in PCSA between synergist muscles as representative of differences in force-generating capacity. However, it is important to note that the PCSA values are sensitive to the joint angle tested. In addition, results cannot be extrapolated to dynamic contractions where activation/force-sharing strategies may be affected by the mechanical constraints of the task (Smith et al., 1980; Wakeling and Horn, 2009). Future research might provide further insights into neuromechanical coupling during dynamic tasks by informing muscle modelling (e.g. Dick et al., 2017) with experimental data (e.g. PCSA, moment arms). Finally, testing was performed with the ankle in the neutral position (0 deg), where we assumed that the three heads of the triceps surae are at a similar muscle length relative to their optimal length. This assumption seems reasonable for GM and GL because their anatomy (Szaro et al., 2009), architecture (Maganaris et al., 1998), composition (Johnson et al., 1973) and ascending parts of their force–length relationships (Maganaris, 2003) are very similar. The comparison between gastrocnemii and the SOL is less straightforward as their composition, anatomy and function differ. However, at 0 deg, gastrocnemii and the SOL both operate in the ascending limb and plateau region of the force–length relationship, with an optimal angle at approximately 15 deg of dorsiflexion for the SOL (Maganaris, 2001) and at 19 deg of dorsiflexion for the GM (Hoffman et al., 2012). Therefore, it seems reasonable to assume that the force imbalance between synergist muscles that we estimated is minimally affected by difference in the operating ranges of the muscles over the force–length relationship.

Conclusions

This study provides insight into the neuromechanical coupling that exists within synergist muscles during an isometric contraction. An important result lies in the consequences of the activation strategies on the imbalance of the force production between synergist muscles, and the high between-individual variability. This large individual variability in the force-sharing strategy raises the question of its

impact on the Achilles tendon. Further studies are required to investigate whether the individual coordination strategies could constitute an intrinsic risk factor to the development of Achilles tendon disorders.

Competing interests

The authors declare no competing or financial interests.

Author contributions

Conceptualization: M.C., L.L., A.N., K.T., F.H.; Methodology: M.C., L.L., A.N., F.H.; Software: M.C., L.L., F.H.; Investigation: M.C., L.L.; Resources: F.H.; Data curation: M.C., F.H.; Writing - original draft: M.C., K.T., F.H.; Writing - review & editing: M.C., L.L., A.N., K.T., F.H.; Supervision: L.L., K.T., F.H.; Project administration: L.L., F.H.; Funding acquisition: F.H.

Funding

This study was supported by a grant from the Région Pays de la Loire (QUETE project, no. 2015-09035). M.C. was supported by a scholarship from the French ministry of higher education and research. F.H. was supported by a fellowship from the Institut Universitaire de France (IUF) and a travel grant from the International French Society of Biomechanics.

Data availability

Data are available from the Dryad Digital Repository (Crouzier et al., 2018): https://doi.org/10.5061/dryad.68jc53n.

References

Ahn, A. N., Kang, J. K., Quitt, M. A., Davidson, B. C. and Nguyen, C. T. (2011). Variability of neural activation during walking in humans: short heels and big calves. *Biol. Lett.* **7**, 539-542.

Albracht, K., Arampatzis, A. and Baltzopoulos, V. (2008). Assessment of muscle volume and physiological cross-sectional area of the human triceps surae muscle *in vivo*. *J. Biomech.* **41**, 2211-2218.

Arndt, A. N., Komi, P. V., Brüggemann, G.-P. and Lukkariniemi, J. (1998). Individual muscle contributions to the *in vivo* Achilles tendon force. *Clin. Biomech.* **13**, 532-541.

Arndt, A., Brüggemann, G.-P., Koebke, J. and Segesser, B. (1999). Asymmetrical loading of the human triceps surae – I. Mediolateral force differences in the Achilles tendon. *Foot Ankle Int.* **20**, 444- 449.

Biewener, A. A. (2016). Locomotion an an emergent property of muscle contractile dynamics. *J. Exp. Biol.* **219**, 285-294.

Bojsen-Møller, J. and Magnusson, S. P. (2015). Heterogeneous loading of the human Achilles tendon *in vivo*. *Exerc. Sport Sci. Rev.* **43**, 190-197.

Bolsterlee, B., Finni, T., D'Souza, A., Eguchi, J., Clarke, E. C. and Herbert, R. D. (2018). Three-dimensional architecture of the whole human soleus muscle *in vivo*. *Peer J* **6**, e4610.

Cresswell, A., Löscher, W. and Thorstensson, A. (1995). Influence of gastrocnemius muscle length on triceps surae torque development and electromyographic activity in man. *Exp. Brain Res.* **105**, 283-290.

Crouzier, M., Lacourpaille, L., Nordez, A., Tucker, K. and Hug, F. (2018) Data from: Neuromechanical coupling within the human triceps surae and its consequence on individual force sharing strategies. Dryad Digital Repository. https://doi.org/10.5061/dryad.68jc53n

Crowninshield, R. D. and Brand, R. A. (1981). A physiologically based criterion of muscle force prediction in locomotion. *J. Biomech.* **14**, 793-802.

Cummins, E. J. and Anson, B. J. (1946). The structure of the calcaneal tendon (of Achilles) in relation to orthopedic surgery, with additional observations on the plantaris muscle. *Surg. Gynecol. Obstet.* **83**, 107-116.

De Troyer, A., Kirkwood, P. A. and Wilson, T. A. (2005). Respiratory action of the intercostal muscles. *Physiol. Rev.* **85**, 717-756.

Dick, T. J. M., Biewener, A. A. and Wakeling, J. M. (2017). Comparison of human gastrocnemius forces predicted by Hill-type muscle models and estimated from ultrasound images. *J. Exp. Biol.* **220**, 1643- 1653.

Diedrichsen, J., Shadmehr, R. and Ivry, R. (2010). The coordination of movement: optimal feedback control and beyond. *Trends Cogn. Sci.* **14**, 31-39.

Dul, J., Johnson, G. E., Shiavi, R. and Townsen, M. A. (1984). Muscular synergism – II. A minimum-fatigue criterion for load sharing between synergistic muscles. *J. Biomech.* **17**, 675-684.

Duysens, J., Tax, A. A. M., van der Doelen, B., Trippel, M. and Dietz, V. (1991). Selective activation of human soleus or gastrocnemius in reflex responses during walking and running. *Exp. Brain Res.* **87**, 193-204.

Edama, M., Kubo, M., Onishi, H., Takabayashi, T., Inai, T., Yokoyama, E., Hiroshi, W., Satoshi, N. and Kageyama, I. (2015). The twisted structure of the human Achilles tendon. *Scand. J. Med. Sci. Sports* **25**, e497-e503.

Farahmand, F., Senavongse, W. and Amis, A. A. (1998). Quantitative study of the quadriceps muscles and trochlear groove geometry related to instability of the patellofemoral joint. *J. Orthop. Res.* **16**, 136-143.

Fiebert, I. M., Spielholz, N. I., Applegate, B., Crabtree, F. G., Martin, L. A. and Parker, K. L. (2000). A comparison of iEMG activity between the medial and lateral heads of the gastrocnemius muscle during partial weight bearing plantarflexion contractions at varying loads. *Isokinet. Exerc. Sci.* **8**, 65-72.

Finni, T., Bernabei, M., Baan, G. C., Noort, W., Tijs, C. and Maas, H. (2017). Non-uniform displacement and strain between the soleus and gastrocnemius subtendons of rat Achilles tendon. *Scand. J. Med. Sci. Sports* **28**, 1009-1017.

Fitts, R. H., Costill, D. L. and Gardetto, P. R. (1989). Effect of swim exercise training on human muscle fiber function. *J. Appl. Physiol.* **66**, 465-475.

Fukunaga, T., Roy, R. R., Shellock, F. G., Hodgson, J. A. and Edgerton, V. R. (1996). Specific tension of human plantar flexors and dorsiflexors. *J. Appl. Physiol.*, 158-165.

Handsfield, G. G., Inouye, J. M., Slane, L. C., Thelen, D. G., Miller, G. W. and Blemker, S. S. (2016). A 3D model of the Achilles tendon to determine the mechanisms underlying nonuniform tendon displacements. *J. Biomech.* **51**, 17-25.

Haxton, H. A. (1944). Absolute muscle force in the ankle flexors in man. *J. Physiol.* **103**, 267-273.

Hedrick, W. R. (2000). Extended field of view real-time ultrasound. *J. Diagn. Med. Sonogr.* **16**, 103-107.

Henneman, E. and Oslon, C. B. (1965). Relations between structure and function in the design of skeletal muscles. *J. Neurophysiol.* **28**, 581-598.

Henneman, E., Somjen, C. and Carpenter, D. O. (1965). Excitability and inhibitability of motoneurons of different sizes. *J. Neurophysiol.* **28**, 599-620.

Héroux, M. E., Dakin, C. J., Luu, B. L., Inglis, J. T. and Blouin, J. S. (2014). Absence of lateral gastrocnemius activity and differential motor unit behavior in soleus and medial gastrocnemius during standing balance. *J. Appl. Physiol.* **116**, 140-148.

Herzog, W. (2000). Muscle properties and coordination during voluntary movement. *J. Sports Sci.* **18**, 141-152.

Herzog, W. (2017). Skeletal muscle mechanics: questions, problems and possible solutions. *J. Neuroeng. Rehabil.* **14**, 98.

Herzog, W. and Leonard, T. R. (1991). Validation of optimization models that estimate the forces exerted by synergistic muscles. *J. Biomech.* **24**, 31-39.

Herzog, W., Read, L. J. and Keurs, H. (1991). Experimental determination of force-length relations of intact human gastrocnemius muscles. *Clin. Biomech.* **6**, 230-238.

Herzog, W., Leonard, T. R. and Guimaraes, C. S. (1993). Forces in gastrocnemius, soleus, and plantaris tendons of the freely moving cat. *J. Biomech.* **26**, 945 - 953.

Hoffman, B. W., Lichtwark, G. A., Carroll, T. J. and Cresswell, A. G. (2012). A comparison of two Hill-type skeletal muscle models on the construction of medial gastrocnemius length-tension curves in humans in vivo. *J. Appl. Physiol.* **113**, 90-96.

Hug, F., Goupille, C., Baum, D., Raiteri, B. J., Hodges, P. W. and Tucker, K. (2015). Nature of the coupling between neural drive and force-generating capacity in the human quadriceps muscle. *Proc. R. Soc. B* **28**2, 20151908.

Johnson, M. A., Polgar, D., Weightman, D. and Appleton, D. (1973). Data on the distribution of fibre types in thirty-six human muscles an autopsy study. *J. Neurol. Sci.* **18**, 111-129.

Kannus, P. (1997). Etiology and pathophysiology of chronic tendon disorders in sports. *Scand. J. Med. Sci. Sports* **7**, 78-85.

Kinugasa, R., Oda, T., Komatsu, T., Edgerton, V. R. and Sinha, S. (2013). Interaponeurosis shear strain modulates behavior of myotendinous junction of the human triceps surae. *Physiol. Rep.* **1**, e00147.

Kutch, J. J. and Valero-Cuevas, F. J. (2011). Muscle redundancy does not imply robustness to muscle dysfunction. *J. Biomech.* **44**, 1264-1270.

Kyrolainen, H. and Komi, P. V. (1994). Stretch reflex responses following mechanical stimulation in power- and endurance-trained athletes. *Int. J. Sports Med.* **15**, 290-294.

Lacourpaille, L., Nordez, A. and Hug, F. (2017). The nervous system does not compensate for an acute change in the balance of passive force between synergist muscles. *J. Exp. Biol.* **220**, 3455-3463.

Larsson, L. and Moss, R. L. (1993). Maximum velocity of shortening in relation to myosin isoform composition in single fibres from human skeletal muscles. *J. Physiol.* **472**, 595-614.

Lieber, R. L. (2002). Skeletal muscle structure, function and plasticity: the physiological basis of rehabilitation. Baltimore: Lippincott Williams & Wilkins.

Maas, H. and Finni, T. (2018). Mechanical coupling between muscle-tendon units reduces peak stresses. *Exerc. Sport Sci. Rev.* **46**, 26-33.

Mademli, L. and Arampatzis, A. (2005). Behaviour of the human gastrocnemius muscle architecture during submaximal isometric fatigue. *Eur. J. Appl. Physiol.* **94**, 611-617.

Maganaris, C. N. (2001). Force-length characteristics of in vivo human skeletal muscle. *Acta Physiol. Scand.* **172**, 279-285.

Maganaris, C. N. (2003). Force-length characteristics of the in vivo human gastrocnemius muscle. *Clin. Anat.* **16**, 215-223.

Maganaris, C. N., Baltzopoulos, V. and Sargeant, A. J. (1998). In vivo measurements of the triceps surae complex architecture in man- implications for muscle function. *J. Physiol.* **512**, 603-614.

Masood, T., Bojsen-Moller, J., Kalliokoski, K. K., Kirjavainen, A., Aarimaa, V., Magnusson, S. P. and Finni, T. (2014). Differential contributions of ankle plantarflexors during submaximal isometric muscle action: a PET and EMG study. *J. Electromyogr. Kinesiol.* **24**, 367-374.

McLean, L. and Goudy, N. (2004). Neuromuscular response to sustained low-level muscle activation: within- and between-synergist substitution in the triceps surae muscles. *Eur. J. Appl. Physiol.* **91**, 204-216.

Noorkoiv, M., Stavnsbo, A., Aagaard, P. and Blazevich, A. J. (2010). In vivo assessment of muscle fascicle length by extended field-of-view ultrasonography. *J. Appl. Physiol.* **109**, 1974-1979.

Pekala, P. A., Henry, B. M., Ochala, A., Kopacz, P., Taton, G., Mlyniec, A., Walocha, J. A. and Tomaszewski, K. A. (2017). The twisted structure of the Achilles tendon unraveled- A detailed quantitative and qualitative anatomical investigation. *Scand. J. Med. Sci. Sports* 1-11.

Prilutsky, B. (2000). Coordination of one-joint and two-joint muscles. *Motor Control* **4**, 1-44.

Riemann, B. L., Limbaugh, G. K., Eitner, J. D. and LeFavi, R. G. (2011). Medial and lateral gastrocnemius activation differences during heel-raise exercise with three different foot positions. *J. Strength Conditionong Res.* **25**, 634- 639.

Sacks, R. D. and Roy, R. R. (1982). Architecture of the hind limb muscles of cats – functional significance. *J. Morphol.* **195**, 173-185.

Smith, J. L., Betts, B., Edgerton, V. R. and Zernicke, R. F. (1980). Rapid ankle extension during paw shakes: selective recruitment of fast ankle extensors. *J. Neurophysiol.* **43**, 612-620.

Szaro, P., Witkowski, G., Smigielski, R., Krajewski, P. and Ciszek, B. (2009). Fascicles of the adult human Achilles tendon – an anatomical study. *Ann. Anat.* **191**, 586-593.

Todd, G., Taylor, J. L. and Gandevia, S. C. (2004). Reproducible measurement of voluntary activation of human elbow flexors with motor cortical stimulation. *J. Appl. Physiol.* **97**, 236-242.

Wakeling, J. M. and Horn, T. (2009). Neuromechanics of muscle synergies during cycling. *J. Neurophysiol.* **101**, 843-854.

Walmsley, B., Hodgson, J. A. and Burke, R. E. (1978). Forces produced by Medial gastrocnemius and Soleus muscles during locomotion in freely moving cats. *J. Neurophysiol.* **41**, 1203-1216.

Whiting, W. C., Robert, J. C., Roy, R. R. and Edgerton, V. R. (1984). A technique for estimating mechanical work of individual muscles in the cat during treadmill locomotion. *J. Biomech.* **19**, 685-694.

Winter, S. L. and Challis, J. H. (2008). Reconstruction of the human gastrocnemius force–length curve *in vivo* – Part 2 – experimental results. *J. Appl. Biomech.* **24**, 207-214.